

Molecular dynamics simulations of oxide memory resistors (memristors)

S. E. Savel'ev¹, A. S. Alexandrov^{1,2}, A. M. Bratkovsky², and R. Stanley Williams²

¹*Department of Physics, Loughborough University,
Loughborough LE11 3TU, United Kingdom*

²*Hewlett-Packard Laboratories, 1501 Page Mill Road, Palo Alto, California 94304*

Abstract

Reversible bipolar nano-switches that can be set and read electronically in a solid-state two-terminal device are very promising for applications. We have performed molecular-dynamics simulations that mimic systems with oxygen vacancies interacting via realistic potentials and driven by an external bias voltage. The competing short- and long-range interactions among charged mobile vacancies lead to density fluctuations and short-range ordering, while illustrating some aspects of observed experimental behavior, such as memristor polarity inversion.

I. INTRODUCTION

Nanoscale metal/oxide/metal two-terminal non-linear circuit elements and switches would be extremely attractive for dense memory, logic, neurocomputing etc if they could scale well in size, power, driving voltage, and can perform without much fatigue in a repeatable and uniform (across e.g. the memory matrix) manner. Some of these issues are not well understood although the hysteretic behavior of such materials, especially thin films of Transition Metal Oxides (TMO) like Ta_2O_5 , Nb_2O_5 , TiO_2 , NiO , Cu_2O , and Group III and IV oxides (Al_2O_3 , SiO_x), in metal-insulator-metal (MIM) vertical devices have been studied for decades [1–8]. The diverse semiconductor[9–11], polymer[12, 13], and correlated oxide systems [10, 14–17] exhibited switching under electric pulsing. In recent years, interest in various oxide-based systems switchable by an electric pulse has grown quite dramatically leading to important breakthroughs and exposing various fundamental problems related to mechanisms of bipolar (driven by alternating positive and negative biasing to close the I-V hysteresis loop) and unipolar (driven by the bias of one polarity) switching behavior [18–20]. In particular, it was realized that bipolar switches are analogous to the ‘memristor’, a fourth passive circuit element originally postulated by Leon Chua in 1971[18].

There are challenges in understanding and controlling the coupled electronic and ionic kinetic phenomena that dominate the behavior of oxide switching devices like $\text{Pt}/\text{TiO}_2/\text{Pt}$, which is an exemplar memristor (resistor with memory)[19]. It has been demonstrated unambiguously that bipolar switching involves changes to the electronic barrier at the Pt/TiO_2 interface due to the drift of positively charged oxygen vacancies under an applied electric field[19]. Various direct measurements revealed formation of localized conducting channels in TiO_2 : pressure modulated conductance microscopy [21, 22], conducting atomic force microscopy (AFM) [23], scanning transmission x-ray microscopy [24, 25], and in-situ transmission electron microscopy [26]. On the basis of these measurements, it became quite clear that the vacancy drift towards the interface creates conducting channels that shunt, or short-circuit, the electronic barrier and switch the device ON[19]. The drift of vacancies away from the interface breaks such channels, recovering the electronic barrier to switch the junction OFF. More recently, Kwon *et al.* [26] have performed the direct cross-sectional TEM studies of the unipolar resistive switching of TiO_2 , revealing the presence of nanoscale Magneli phase Ti_4O_7 conductive channels following device turning on and imaging the fila-

ment region in TEM. A Ti_4O_7 phase was confirmed from the temperature dependence of the conductance. Concurrently, Strachan *et al.* [24, 25] investigated the bipolar mode of TiO_2 switching, using non-destructive spatially-resolved x-ray absorption and electron diffraction that allows nanometer scale studies of the associated chemical and structural changes of a functioning memristive device. They have observed that electroforming of the device is accompanied by forming an ordered Magneli phase channel within the initially deposited (amorphous) TiO_2 matrix.

The observation of a Magneli crystallite in a titanium dioxide matrix shows that electroforming Pt/ TiO_2 /Pt memristive system is related to a localized partial reduction of titanium dioxide and crystallization of a metallic conducting channel Ti_4O_7 . Inside a titanium dioxide matrix, the Magneli phases are thermodynamically favored over a high concentration of randomly distributed vacancies, and thus they can act as a source or sink of vacancies in the matrix material depending on the electrochemical potential within the device[27]. The application of an electrical bias can control vacancy motion in and out of this sub-oxide phase, modulating a transport barrier and leading to the dramatic conductivity change. It is worth noting that hysteretic switching in some perovskite oxides monitored by TEM did not show any indication of conducting channel formation [28]. Therefore, two types of models are usually considered (i) in-plane homogeneous and (ii) in-plane inhomogeneous changes accompanying switching in the material[7]. We shall study the kinetics of oxygen vacancies in a generic situation like TiO_2 by way of molecular dynamics to visualize processes taking place at the atomic scale that are reminiscent of actual device behavior and whose origin is in competing vacancy-vacancy interactions.

Another important aspect is that the forming step for the channel formation in systems like TiO_2 , NiO , VO_2 is accompanied by local heating that is witnessed by the local emergence of high-temperature phases and observed by thermal microscopy. It is worth noting that bipolar switching is apparently field-driven and is very different from unipolar switching that is power-driven. As a result, the bipolar switches may consume much less power than the unipolar switches. At the same time, local heating does accompany and seems to be important in both processes. Thus, fresh TiO_2 samples have an amorphous layer of titanium dioxide. To make the device switch in a repeatable manner, a *forming step* of rather large voltage pulse is usually required to create a vacancy-rich region (forming is not required if e.g. a vacancy-rich layer is provided intentionally by fabrication). During

this process, the TiO_2 anatase phase forms near the conducting channel, which nominally requires temperatures over 350°C [25]. Studying local thermal effects during switching in TiO_2 provides strong evidence for local heating [29]. Unambiguous evidence for local heating accompanying conducting channel formation comes from third harmonic generation [30]; low resistance states (LRSs) in NiO showing *unipolar* switching were strongly nonlinear with variations in the resistance R as large as 60%, which was most likely caused by the Joule heating of conducting channels inside the films. One can note at this point that since the *unipolar* switching is power driven, therefore, it may be problematic to use it because of power requirements.

Given the above, the microscopic understanding of the atomic-scale mechanism and identification of the material changes within an insulating barrier appears to be invaluable for controlling and improving the memristor performance. Within the volume $10\times10\times2\text{ nm}^3$ of perspective nano-memristors the number of oxygen vacancies could be as small as a thousand, so that the conventional statistical approach for dealing with many-particle systems might fail. Many important phenomena such as dynamic phase transitions, as well as competition between thermal fluctuations and particle-particle interactions in stochastic transport, can be investigated using the Molecular Dynamics (MD) simulations of the Langevin equations describing the thermal diffusion and drift of individual interacting particles [31]. Here we present some preliminary results of such simulations for a model memristor.

II. MODELING A MEMRISTOR

In a semiconducting titanium dioxide, oxygen vacancies play an important role in the electrical conduction. A stoichiometric TiO_2 crystal is a colorless and transparent insulator. However, heated in vacuum, it loses a part of its oxygen, or is reduced, and becomes dark blue in color and electrically conductive. At high temperatures about 1000 C ionic conduction becomes observable originating from oxygen and titanium vacancies [32] while at ambient and lower temperatures small polarons carry the current [33]. The reduced rutile shows an anomalous electrical property under a DC electric field of several tens of V/cm [32]. When a DC electric field was applied to the bulk sample of reduced TiO_2 , a single pulse of electric current was observed together with a constant background current. This pulsed current has been attributed to migration of oxygen vacancies in reduced TiO_2 under a DC electric field.

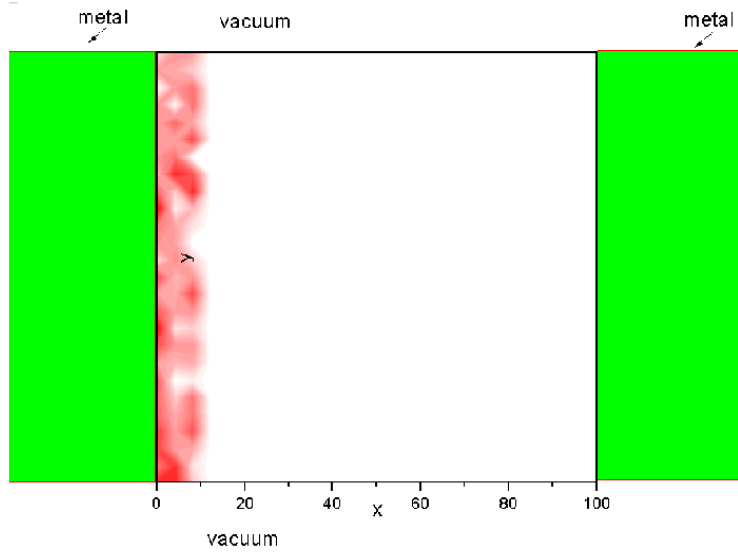


FIG. 1: (Color online) Model oxide memristor with a reduced oxygen layer near one of the metallic leads (the length scale is arbitrary)

The oxygen migration is visually observable under a DC electric field. Namely, when a DC electric field was applied to the sample after repeated change of its polarity, the color of the sample around the negative electrode changed into dark blue due to the higher density of oxygen vacancies, while the region around the positive electrode lost color [32]. In order to explain these features, Miyaoka *et al.* [32] have proposed that the oxygen vacancies form clusters under a voltage, which may create crystalline phases different from rutile, namely Magneli phases, as recently observed in nanoscale probes[25, 26].

Based on the observations of oxygen vacancy migration and clustering in bulk [32] and nanoscale [25, 26] samples of TiO_2 induced by an electric-field, we model a memristor as shown in Fig. 1. In our model, there is a reduced rutile thin layer TiO_{2-x} near one of the metallic electrodes stabilized by the Coulomb mirror potential. Vacancies from this layer can drift toward the opposite electrode in an electric field.

The simplest approach to the vacancy diffusion is using a drift-diffusion equation for the

density of vacancies $n(\mathbf{x}, t)$,

$$\frac{\partial n(\mathbf{x}, t)}{\partial t} = D \left[\frac{\partial^2 n(\mathbf{x}, t)}{\partial \mathbf{x}^2} - \frac{\mathbf{F}(t)}{k_B T} \frac{\partial n(\mathbf{x}, t)}{\partial \mathbf{x}} \right], \quad (1)$$

which neglects the particle-particle interaction. Here D is the diffusion coefficient, T is the temperature, and $\mathbf{F}(t)$ is the electric field. The diffusion equation (1) can be mapped onto a simple Langevin equation

$$\frac{dx_i^\alpha}{dt} = F^\alpha(t) + \sqrt{D^\alpha} \xi_i^\alpha(t), \quad (2)$$

where $\alpha = x, y, z$ Cartesian components, $\vec{\xi}$ is a stochastic force of zero mean and δ -correlated in time, and we accounted for anisotropic diffusion (in TiO_2 rutile diffusion along the c-axis is much faster than in ab-plane, for instance).

With the use of the standard Euler method[31], we have simulated one thousand vacancies ($i = 1, \dots, 1000$). The result is shown in Fig.2 for a rectangular electric pulse, $F(t)$. There is no clustering in this simple diffusion approximation, but rather uniform propagation of the reduced layer accompanied by its widening in the propagation direction, which is the same as the analytical result in this case.

III. MOLECULAR DYNAMICS OF INTERACTING VACANCIES

Now let us simulate the stochastic transport of vacancies fully taking into account their interaction and boundary conditions. We consider an open system of N point-like Brownian vacancies interacting with each other via the pairwise potential W , with a possible inclusion of the substrate through some periodic and random potentials U , and with internal and external fields corresponding to the time-dependent deterministic force F . The environment exerts an independent Gaussian random force, $\vec{\xi}$ on each particle with zero mean and intensity controlled by the temperature. In the overdamped regime (where inertia is negligible compared to the viscous damping), the Langevin equation describing the drift-diffusion of the i -th particle is [31]:

$$\eta \frac{dx_i^\alpha}{dt} = F_i^\alpha(\mathbf{x}_i, t) - \sum_{j \neq i} \frac{\partial W(\mathbf{x}_i - \mathbf{x}_j)}{\partial x_i^\alpha} + \sqrt{2k_B T \eta} \xi_i^\alpha(t). \quad (3)$$

The unit of $\vec{\xi}_i$ is $s^{-1/2}$. The physical unit of length is the thickness of the memristor, L , (about or less than 5 nm). Then the physical unit of time is L^2/D , where $D = k_B T / \eta$.

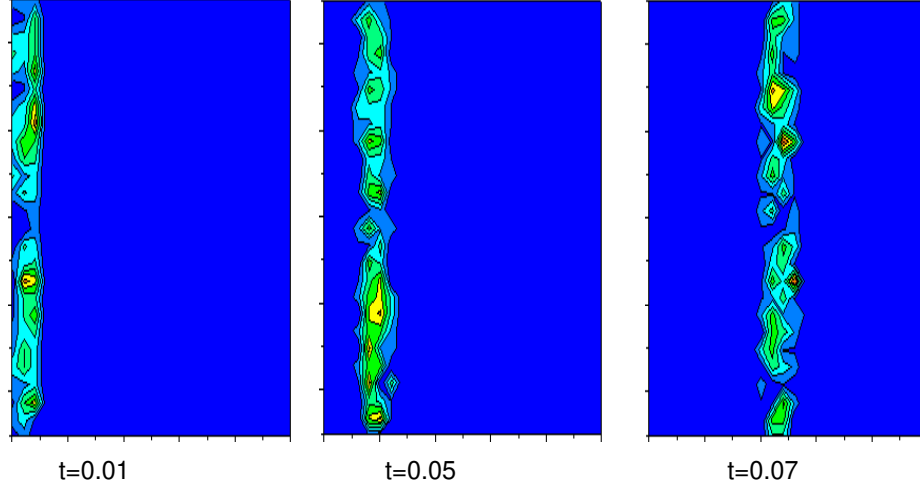


FIG. 2: (Color online) Simulated vacancy motion under the electric pulse governed by the simplest diffusion equation (1) showing no clustering (length and time scales are arbitrary)

(we take the largest D for anisotropic TiO_2). The diffusion coefficient D should be taken at a local temperature, but we have assumed some net temperature across the active area in order to simplify matters in the present simulation. Using the dimensionless time $\tau = tD/L^2$ and dimensionless coordinates $\mathbf{r}_i = \mathbf{x}_i/L$, the equations (3) can be written as

$$\frac{dr_i^\alpha}{d\tau} = -\frac{\partial[V(\mathbf{r}_i, \tau) + U(\mathbf{r}_i)]/(k_B T)}{\partial r_i^\alpha} - \sum_{j \neq i} \frac{\partial W(\mathbf{r}_i - \mathbf{r}_j)/(k_B T)}{\partial r_i^\alpha} + \sqrt{2}\xi_i^\alpha(\tau), \quad (4)$$

where $V(\mathbf{r}_i, \tau)$ is the electric-field potential, and the components of the (dimensionless) random force, ξ_i^α ($\alpha = x, y, z$), satisfies the fluctuation - dissipation relation $\langle \xi_i^\alpha(0)\xi_j^\beta(\tau) \rangle = \delta(\tau)\delta_{\alpha,\beta}\delta_{i,j}$. Diffusion in TiO_2 is strongly anisotropic, thus the diffusion along the c-axis and in-plane will be described by two equations with different diffusion coefficients in more accurate simulations.

The set of equations (4) is equivalent to an infinite BBGKY (Bogoliubov - Born - Green - Kirkwood - Yvon hierarchy) set of equations for multi-particle distribution functions. With no particle-particle interaction it reduces to the drift-diffusion equation (1). Also, in a mean

field approximation, one obtains an additional drift term in the diffusion equation, which however does not lead to clustering.

The O^{2-} vacancy-vacancy interaction potential, which is crucial for their clustering and phase transformations, can be modeled as

$$W(R) = A \exp(-R/a) - B/R^6 + e^2/(\pi\epsilon_0\epsilon R), \quad (5)$$

where the short-range repulsive and attractive parts are represented with $A = 22764.0$ eV, $a = 0.01490$ nm, and $B = 27.88 \times 10^{-6}$ eV nm [34], and the long-range Coulomb repulsion is the last term. More generally the interaction parameters A, B, a vary from one oxide to another, and the dielectric constant ϵ may also vary from sample to sample.

To estimate the diffusion coefficient one can use an empirical equation of Ref. [35],

$$D [\text{cm}^2/\text{s}] = (1.03 \times 10^{-3}) \exp(-E_v/k_B T), \quad (6)$$

where the activation energy for oxygen vacancy diffusion has a poorly known value, with estimates ranging from 0.5 eV to about 1.1 eV. The lower boundary, $E_v = 0.5$ eV, corresponds to $D \approx 3.44 \times 10^{-12}$ cm²/s at the room temperature. For higher activation energies, the vacancies would be immobile, as they are known to be at room temperature. We do know, however, that they move during switching. In this regard, it is worth noting that (i) another important parameter is the local temperature during switching and (ii) strong local electric field concentration at the tips of conducting channels/filaments. Some estimates indicate that the local temperature may reach values like 650K, in which case the diffusion coefficient would be much larger, obviously. The local field concentration near tips of conducting channels/filaments is another variable that will very strongly facilitate the growth of the channel and needs to be simulated self-consistently along with local heating.

Given the uncertainties with ionic diffusion in memristors, at this stage we would restrict ourselves to qualitative and semi-quantitative analysis. The following parameters are chosen at this stage more for computational convenience than to model actual devices. In actual devices the voltage drop across the active region may be moderate, on the order of 1V, and the pulse duration for switching may be just a few microseconds. With $L = 5$ nm and such diffusion coefficient the time unit is $L^2/D \approx 0.7$ ms. The electric pulse rising time 100 ns would correspond to $\tau_r = 1.4 \times 10^{-4}$ and an pulse length 10 μ s corresponds to $\tau_{imp} = 1.4 \times 10^{-3}$. The pulse amplitude of 5 V would then yield the dimensionless force

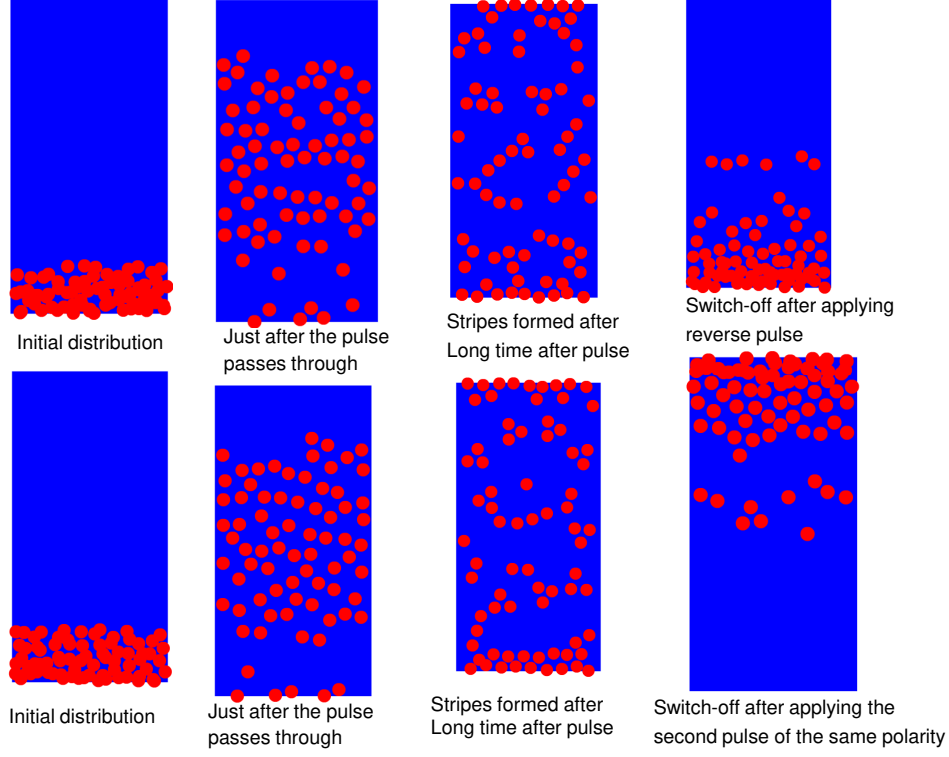


FIG. 3: (Color online) Two successive runs (upper and lower panels, respectively) of the toy-model simulations with periodic BC and parameters described in the text. The bottom panel illustrates the “polarity inversion” of the vacancies from bottom to top electrode during successive pulsing. Analogous behavior has been observed experimentally in Ref.[36].

$F \equiv eV/(k_B T) \approx 200$ at room temperature. The characteristic particle speed is $v = eV/L\eta$, so that the dimensionless collision time is $\tau_{col} = a/LF \approx 1.5 \times 10^{-5}$, and the number of computing steps is $1/\tau_{col} \approx 70000$, representing a challenge for MD simulations. The characteristic collision distance R_c , where the collision force changes its sign from attraction to repulsion, is in fact several times larger than a , which makes the number of MD steps manageable. Also, decreasing the electric pulse amplitude makes the number of the MD steps smaller. We will present simulations for more realistic parameters elsewhere, with the inclusion of local thermal effects directly into simulations.

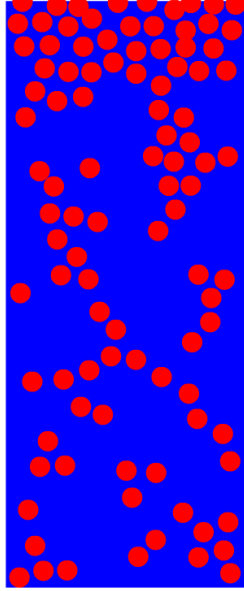


FIG. 4: (Color online) The same as in Fig. 3 with a trend towards formation of a percolation path along the chains of oxygen vacancies.

IV. MD SIMULATION OF A TOY MEMRISTOR: CLUSTERING OF VACANCIES

In view of those uncertainties, we present here the MD simulations of a toy memristor with relatively small number of vacancies, $N = 75$ (Fig. 3) and 150 (Fig. 4), leaving simulations of real devices for future studies. Initially, we have randomly placed all the vacancies near the bottom of a toy sample (see Fig. 3 for initial distribution panels) and then let these vacancies evolve according to Eq.(4) inside a rectangular box which mimics either a part (Figs. 3, 4) or the entire (Fig. 5) sample. We use the 2D simulation area with aspect ratio $L_y/L_x = 2$ (Figs. 3,4) and $4/3$ (Fig. 5) and either periodic boundary conditions (BC) (Fig.3, 4) or impenetrable boundaries (Fig.5) along the x-direction. Note that periodic BC allow us to simulate a quite large sample using a rather small number of particles, while the impenetrable BC can elucidate the role of boundaries or 1D defects in a real finite size sample. To simulate periodic BC, we include periodic images of vacancies with

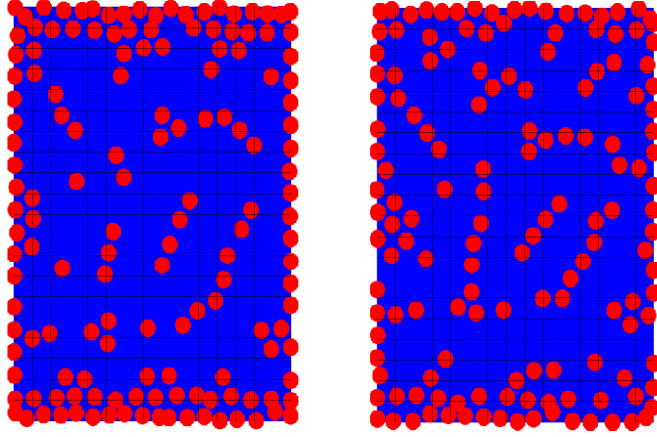


FIG. 5: (Color online) Results of toy-model simulations of a system with impenetrable boundaries and parameters described in the text. As in Fig. 3, one can see clustering of Oxygen vacancies. Moreover, the sample boundary pins vacancies, favoring the formation of percolation paths at the edges of the sample. The left and right panels correspond to two successive runs with the same parameters but different initial vacancy distributions. The observed edge effect is very reminiscent of some memristors where switching areas tend to form near edges[25].

respect to vertical boundaries of the simulation box. We also incorporate opposite polarity charges by adding mirror images of vacancies with respect to the top and the bottom of the sample. Since we simulate a limited number of vacancies, one can refer to each particle in our simulations as a cluster of vacancies, where a cluster-cluster interaction described by the combination of the Lennard-Jones and Coulomb potentials acting with the force

$$F(r) = \frac{1}{r} \left\{ 12E_{LJ}[(r_{min}/r)^{12} - (r_{min}/r)^6] + E_c r_{min}/r \right\}, \quad (7)$$

the relative strength of the Coulomb potential $E_c/E_{LJ} = 2$ and the potential well is about $30k_B T$. This results in the position of the potential maxima $r_{max} \approx 2r_{min}$ and the height of the potential barrier on the order of the depth of the potential well. The pulse strength is

taken to be about 10 times stronger than the maximum attracting force between vacancy clusters.

The results of our toy-modeling look very promising. We see that pulsing in opposite directions initially pushes the vacancies towards the top electrode and then back, Fig.3. Pulsing twice in the forward direction moves the vacancies from the bottom to the top electrode, thus inverting the vacancy distribution in close analogy to what has been done experimentally[36]. We observe a complex kinetics of the oxygen vacancies in all present simulations. In particular, we have observed fragmentation of vacancy distribution and formation of the short vacancy chains for both the periodic and impenetrable boundary conditions. One can envisage that in certain conditions those chains may form percolation paths (Fig. 4), facilitated by e.g. pinning centers and/or boundaries of the sample. Further studies would elucidate the conditions under which a conducting channel may emerge in the sample driven by E-field, thus gaining more insight into the switching of memristors.

V. CONCLUSIONS

We have proposed a model for the kinetic behavior of oxide memristors and simulated its toy analog using the Molecular Dynamics Langevin equations. Our MD simulations reveal a significant departure of the vacancy distributions across the device from that expected within a standard drift-diffusion approximation, driven by interactions among the mobile ionic species (oxygen vacancies in TiO_2 , as a generic example). A realistic vacancy-vacancy interaction incorporating short and long-range repulsions along with a medium-range attraction leads to clustering of vacancies into chains. This may shed new light onto conducting channel formation in memristors. We have found a significant effect of boundaries on the clustering patterns. MD experiments (before averaging over configurations) have the potential to simulate conditions that are hard or even impossible to incorporate in the standard drift-diffusion models, such as the vacancy annihilation or generation (from the air), different shapes of boundaries, vacancy pinning (either periodic or random) and an inhomogeneous external field (due to edge effects etc.). One can also calculate not only the density distribution but binary distributions, velocity distributions etc., providing any desired statistical analysis of the distributions. Another important step would be to include thermal effects via local changes in the anisotropic diffusion coefficient. Competing interactions between mo-

bile ionic species are seen as a robust mechanism for vacancy concentration fluctuations and clustering, which shows that switching in real devices is a statistical or stochastic process.

-
- [1] G.S. Kreynina, L.N. Selivanov, and T.I. Shumskaya, *Radio Eng. Electron.* **5**, 219 (1960).
 - [2] G.S. Kreynina, *Radio Eng. Electron.* **7**, 1949 (1962).
 - [3] J.F. Gibbons and W.E. Beadle, *Solid-State Electron.* **7**, 785 (1964).
 - [4] K. L. Chopra, *J. Appl. Phys.* **36**, 184 (1965).
 - [5] F. Argall, *Solid-State Electron.* **11**, 535 (1968); H. Schroeder and D.S. Jeong, *Microelectr. Engin.* **84**, 1982 (2007).
 - [6] T.W. Hickmott and W.R. Hiatt, *Solid-State Electron.* **13**, 1033 (1970).
 - [7] G. Dearnaley, A.M. Stoneham, and D.V. Morgan, *Rep. Prog. Phys.* **33**, 1129 (1970).
 - [8] D.P.Oxley, *Electrocomponent Sci. Technol.* **3**, 217 (1977).
 - [9] S. R. Ovshinsky, *Phys. Rev. Lett.* **21**, 1450 (1968); S. R. Ovshinsky and H. Fritzsche, *IEEE Trans. Electron. Dev.* **ED-20**, 91 (1973); G.W. Burr *et al.*, *J. Vac. Sci. Technol. B* **28**, 223 (2010).
 - [10] P.W.M. Blom, R.M. Wolf, J.F.M. Cillessen, and M.P.C.M. Krijn, *Phys. Rev. Lett.* **73**, 2107 (1994).
 - [11] H. Akinaga *et al.*, *IEEJ Trans. Electr. Electron. Engin.* **2**, 453 (2007).
 - [12] V. I. Stafeev, V. V. Kusnetsova, V. P. Molchanov, E. I. Karakashan, S. V. Airapetyants, and L. S. Gasanov, *Sov. Phys. Semicond.* **2**, 647 (1968).
 - [13] W. P. Ballard and R. W. Christy, *J. Non-Cryst. Solids* **17**, 81 (1975).
 - [14] S. Thakoor, A. Moopen, T. Daud, and A.P. Thakoor, *J. Appl. Phys.* **67**, 3132 (1990).
 - [15] A. Asamitsu, Y. Tomioka, H. Kuwahara, and Y. Tokura, *Nature* **388**, 50 (1997).
 - [16] A. Beck, J.G. Bednorz, Ch. Gerber, C. Rossel, and D. Widmer, *Appl. Phys. Lett.* **77**, 139 (2000).
 - [17] Y. Watanabe, J.G. Bednorz, A. Bietsch, Ch. Gerber, D. Widmer, A. Beck, and S.J. Wind, *Appl. Phys. Lett.* **78**, 3738 (2001).
 - [18] D. B. Strukov, G. S. Snider, D. R. Stewart, and R. S. Williams, *Nature* **453**, 80 (2008).
 - [19] J.J. Yang, M.D. Pickett, X.M. Li, *et al.* *Nature Nanotech.* **3**, 429 (2008).
 - [20] R. Waser, R. Dittmann, G. Staikov, and K. Szot, *Adv. Mater.* **21**, 2632 (2009).

- [21] J. J. Yang, F. Miao, M. D. Pickett, D. A. A. Ohlberg, D. R. Stewart, C. N. Lau, and R. S. Williams, *Nanotechnology* **20**, 215201 (2009).
- [22] F. Miao, J. J. Yang, J. P. Strachan, D. Stewart, R. S. Williams, and C. N. Lau, *Appl. Phys. Lett.* **95**, 113503 (2009).
- [23] R. Mustermann, J. Yang, J. P. Strachan, G. Medeiros-Ribeiro, R. Dittmann, and R. Waser, *Phys. Stat. Sol. (RRL)* **4**, 16 (2009).
- [24] J. P. Strachan, J. J. Yang, R. Mustermann, A. Scholl, G. Medeiros-Ribeiro, D. R. Stewart, and R. S. Williams, *Nanotechnology* **20**, 215201 (2009).
- [25] J. P. Strachan, M. D. Pickett, J. J. Yang, S. Aloni, A. L. D. Kilcoyne, G. Medeiros-Ribeiro, and R. S. Williams, *Adv. Mater.* **22**, 3573 (2010).
- [26] D.-H. Kwon, K. M. Kim, J. H. Jang, J. M. Jeon, M. H. Lee, G. H. Kim, X.-S. Li, G.-S. Park, B. Lee, S. Han, M. Kim, C. S. Hwang, *Nat. Nanotech.* **5**, 148 (2010).
- [27] L. Liborio, G. Mallia, and N. Harrison, *Phys. Rev. B* **79**, 245133 (2009); L. Liborio and N. Harrison, *Phys. Rev. B* **77**, 104104 (2008).
- [28] T. Fujii, H. Kaji, H. Kondo, K. Hamada, M. Arita, and Y. Takahashi, *IOP Conf. Ser.: Mater. Sci. Engin.* **8**, 012033 (2010).
- [29] J. Borghetti, D. B. Strukov, M. D. Pickett, J. Yang, D. R. Stewart, and R. S. Williams, *J. Appl. Phys.* **106**, 124504 (2009). nohT07 : J. S. Lee, M. Ortolani, U. Schade, Y. J. Chang, and T. W. Noh, *Appl. Phys. Lett.* **90**, 051907 (2007); *ibid.* **91**, 133509 (2007).
- [30] S. B. Lee, S. C. Chae, S. H. Chang, J. S. Lee, S. Park, Y. Jo, S. Seo, B. Kahng, and T. W. Noh, *Appl. Phys. Lett.* **93**, 252102 (2008).
- [31] S. Savel'ev, F. Marchesoni, and F. Nori, *Phys. Rev. E* **70**, 061107 (2004), and references therein.
- [32] H. Miyaoka, G. Mizutani, H. Sano, M. Omote, K. Nakatsuji, and F. Komori, *Sol. State Commun.* **123**, 399 (2002); K. Tsunoda *et al.*, *Appl. Phys. Lett.* **90**, 113501 (2007); K. M. Kim *et al.*, *Appl. Phys. Lett.* **90**, 242906 (2007); J. R. Jameson *et al.*, *Appl. Phys. Lett.* **91**, 112101 (2007); H. Shima *et al.*, *Appl. Phys. Lett.* **94**, 082905 (2009); Ni Zhong *et al.*, *Appl. Phys. Lett.* **96**, 042107 (2010); and references therein.
- [33] A. S. Alexandrov and N. F. Mott, *Polarons and Bipolarons* (World Scientific, Singapore-London, 1995), p.156.
- [34] C. Meis and J. L. Fleche, *Solid State Ionics* **101**, 333 (1997).

- [35] M. Radecka, P. Sobas, and M. Rekas, Solid State Ionics **119**, 55 (1999).
- [36] J.J. Yang, J. Borghetti, D. Murphy, D.R. Stewart, and R.S. Williams, Adv. Mater. **21**, 1 (2009).